Quantification of Visible Aerosols from Pyrotechnics: The Effect of Relative Humidity

Rene Yo Abe,[a] Yoshiaki Akutsu,[a] Akihiro Shimada[b] and Takehiro Matsunaga [b]

[a] Department of Environment Systems, Graduate School of Frontier Sciences, The University of Tokyo, 5-1-5 Kashiwanoha Kashiwa, Chiba 277-8563, Japan. Fax: (+) 81-4-7136-4729, email: abe@geel.k.u-tokyo.ac.jp

[b] Research Institute of Science for Safety and Sustainability, National Institute of Advanced Industrial Science and Technology, 1-1-1 Higashi, Tsukuba 305-8565, Japan

Abstract: *Light transmission and particle size distribution measurements of aerosol (smoke) emissions from pyrotechnic compositions have been performed in a combustion chamber at atmospheric pressure over a wide range of relative humidity. Maximum light extinction over time is proportional to weight of incinerated sample and shows a characteristic curve over relative humidity for each pyrolant. When critical relative humidity is exceeded, a distinct increase in light extinction is observed, which can mostly be attributed to enhancement of the light-scattering efficiencies of submicrometer particles by hygroscopic growth thereof. The proposed measurement method allows humidity characteristics of pyrotechnic smoke emissions to be compared.*

1. Introduction

Through interaction with humidity in ambient air, combustion products of pyrotechnics can produce dense smoke-plumes, i.e. aerosols. For fireworks, reduction of adverse effect on visibility is of particular interest, because ongoing displays can be obscured under high humidity and low wind conditions. Even supposedly smoke-free compositions like ammonium perchlorate (AP)/ hydroxyl-terminated polybutadiene (HTPB), which is used as propellant in some rocket motors, develop visually obscuring aerosols from the gaseous combustion products under high humidity conditions.[1] Though the production of visible aerosol is intended in some applications (e.g. smoke screens or signaling),[2,3] it is undesirable in firework scenes especially if increased by humidity. Especially in the Asian region, very high humidity conditions tend to occur often during the warm season which is when firework festivals are mostly held.

Solid hygroscopic particles in aerosols can grow by condensation of water to form aqueous droplets when critical relative humidity is exceeded. The effect of relative humidity on particle growth is well known for a number of substances.[4,5] HCl emissions from chlorine based oxidants like perchlorates, which are commonly used in pyrotechnics, also cause mists to be produced in high humidity or low temperature conditions.[1,6] In the presence of HCl vapor, condensation on hygroscopic particles is further promoted to produce even denser smoke clouds.

Light scattering by aerosol particles reduces contrast and brilliance, i.e. visibility of pyrotechnics. Attenuation of straight light transmittance through aerosol clouds and addition of scattered light to an otherwise generally dark background both degrade the visual impression of pyrotechnics. Most conceivable combustion products except soot can be described as transparent particles with refractive indices of about 1.33 to 1.5. For such particles, scattering efficiency increases greatly for visible light ($\lambda \approx 0.5$ µm) when diameters grow to around 1 µm.[7,8] Particle size and growth characteristics of therefore make up important factors in describing the optical depth of aerosol emissions.

Although efforts are made to develop compositions and substances that produce reduced visible aerosol (smokeless) emissions,[1,2,9,10] the effect of relative humidity has not yet adequately been characterized. Studies on aerosol emissions from pyrotechnics based on field measurements[11–13] at outdoor pyrotechnic displays, where relative humidity cannot adequately be adjusted, or on confined volume experiments,[14,15] mostly do not include experiments at high humidity conditions. Particle sizes reported in the range of a few hundred nm can however increase significantly by uptake of water vapor from humid ambient air.

Visible aerosol development after combustion of pyrotechnics in ambient air of arbitrary relative humidity can be simulated in chamber experiments. Gas and particulate emissions are quickly diluted and cooled in air and undergo nucleation, coagulation and condensation processes. In this work, a measurement method using a small-scale combustion-chamber is proposed for quantification of visual obstruction by aerosols. This allows comparison of visible aerosol development after combustion of different types of pyrotechnic compositions over a range of controlled humidity conditions. Humidity characteristics of the following three types of pyrotechnic compositions were measured to illustrate typical differences in aerosol visibility: ammonium and potassium perchlorate (AP, KP) based compositions which are widely used as a basis for

Article Details | *Article No:- 109*
Manuscript Received:- 07/07/2014 | *Final Revisions:- 07/12/2014*
Publication Date:- 07/12/2014 | *Archive Reference:- 1735*

pyrotechnic compositions;[16] black powder (BP) which is still the predominant composition used as lifting charge, although it is well known for producing relatively dense aerosols.

2. Experimental

2.1 Pyrotechnic compositions

As a representation of pyrotechnic compositions used in fireworks, the perchlorate based composite formulations presented in Table 1 were used. Application of ammonium perchlorate (AP) and potassium perchlorate (KP) mixed with hydroxyl-terminated polybutadiene (HTPB) binder enabled easy laboratory scale production. Further, grain black powder (75% potassium nitrate, 15% charcoal, 10% Sulfur; Kayaku Japan Co., Ltd) was used as a representative chlorine free pyrotechnic composition. Combustion times varied from instantaneous combustion for black powder up to ten seconds for KP composites. The temperature inside the combustion chamber increased less than 1.0 K per gram combusted sample after combustion, but returned to within 0.2 K above initial conditions in a few minutes due to radiative and convective heat transfer to the surrounding room.

Table 1. *Formulations of composites based on perchlorates*

Symbol	Oxidant		Binder (fuel)
	AP	KP	HTPB + Curing agent
A	82%		18%
K		84%	16%

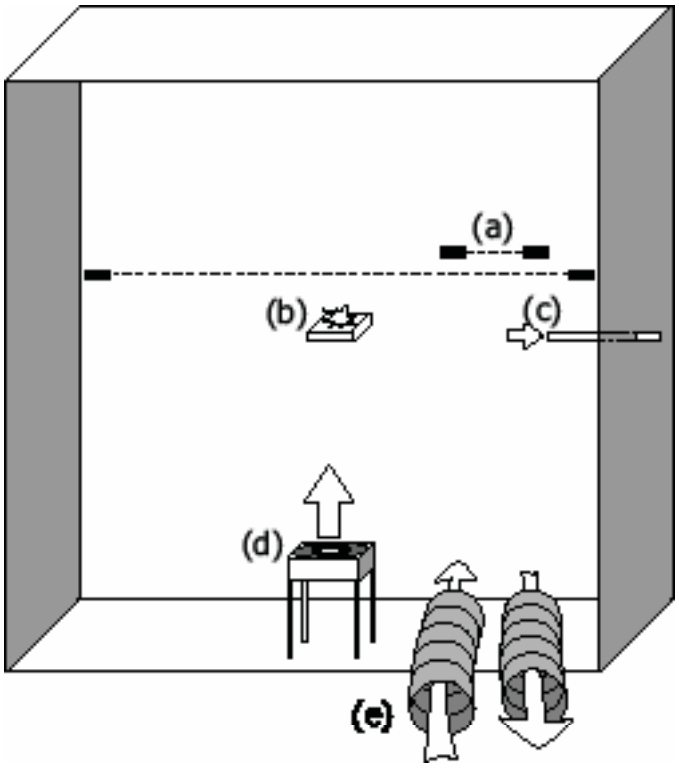

Figure 1. *Combustion chamber features (front view). (a) Laser emitter–transmittance sensor assemblies; (b) combustion platform; (c) sample suction port; (d) circulation fan and psychrometer; (e) ducts to humidity control unit.*

2.2 Combustion chamber

A chamber consisting of a cubic steel frame covered with acrylic sheets at the top and three sides, a stainless steel floor and a detachable soft PVC sheet at the front side was constructed as shown in Figure 1. Room temperature was controlled by air conditioning. After initial temperature and humidity conditions were applied with a humidity controllable type air-conditioning unit (Apiste PAU300S-HC), the chamber was sealed. Combustion experiments were mainly performed at 20 °C, but measurements were also made at 30 °C and for BP also at 10 °C. The air in the chamber was mixed using an electric fan so that a sufficiently homogeneous aerosol was yielded within about ten seconds.

Air temperature and relative humidity inside the chamber were measured near the circulation fan using a psychrometer (measurement of dry-bulb and wet-bulb temperature). This measurement method was easy to maintain and avoided any drifting effects which corrosive gases or aerosol particles emitted by most composites may cause in other humidity sensors. A continuous drip of distilled water kept the wet bulb free of contamination and the whole assembly could be cleaned quickly. Calculation formulae published by the World Meteorological Organization[17] were used to obtain relative humidity values.

2.3 Aerosol opacity and particle size distribution

To evaluate the opacity of the aerosol, light transmittance was monitored during combustion experiments with two laser sensors (Keyence LX-100, λ = 670 nm) installed in the middle of the chamber at distances of 77.5 and 10 cm between emitter and sensor, respectively. The sensor and emitter windows were protected from any aerosol depositions by a flow of clean air which had been passed through a HEPA filter by a membrane pump (RH <60% from outside of the chamber). Two grams of sample per cubic meter were found to be optimal for producing an adequate response in the scattering coefficient over the whole humidity range while not inflating the front chamber cover too much.

The visibility of an aerosol is caused by light scattering or absorption and is dependent on its particle size and number concentration. Combustion products found in aerosol particles can be considered mainly to consist of solid salts or oxides and aqueous solutions of salts and acids which have refractive indices in the range of n_r = 1.33 to 1.5 (real part) for visible light ($\lambda \approx 0.5$ µm). Such particles only show minimal light absorption (imaginary part of refractive index), unless soot particles or special dye substances (colored smoke compositions) are present, or they grow very large as in precipitating clouds. Single particle scattering efficiencies can be described by Mie scattering theory for

small spherical particles ($0.03\lambda < d < 32\lambda$) and scatter visible light ($\lambda \approx 0.5$ µm) most efficiently with particle diameters between 0.3 and 2 µm.[7,8] Particles which are much smaller than the wavelength of light ($d < 0.03\lambda$) are in the Rayleigh regime and absorb or scatter light only weakly. For larger particles, scattering efficiencies also decrease with number concentrations because mass concentrations are limited by condensable vapors.

Particle size distributions (PSD) of aerosols generated by pyrotechnics were reported in previous research to be found in the range of several hundreds of nm.[11,13,14] The visible increase of smoke development in high humidity conditions, however, suggests further growth of hygroscopic particles. Because aerosol concentrations quickly exceeded the measurable range of 10^6 particles per liter, PSD measurements using an optical particle counter (RION KC-11) were only possible with extremely small amounts of sample in the order of tens of mg. This made complete combustion difficult and changes in light-transmittance hardly measurable under conditions which would allow the simultaneous application of particle counting techniques as was previously also observed in large scale chamber experiments.[15]

To measure the PSD of highly concentrated aerosols generated in the chamber, a HORIBA LA-920 particle size distribution analyzer was modified to introduce the aerosol in a sheath flow into a flow cell for measurement of its Mie light scattering pattern. This allowed direct measurement of the aerosol's PSD without prior dilution. Calculation parameters for Mie scattering calculations in particle size measurements with the particle size distribution analyzer were performed using the refractive indices of water and air at 20 °C ($n_r = 1.33$ $n_i = 1.0 \times 10^{-9}$). Simple analysis of scattering patterns with Mie scattering codes[18,19] shows that scattering patterns change greatly with particle size (d = 0.1–10 µm), but not noticeably with refractive indices in the expected range (n_r = 1.33–1.50). Therefore, deviation of actual refractive indices from those used for Mie-scattering pattern analysis does not largely affect calculated PSDs. Also, overall scattering efficiencies can be considered practically constant in the range of refractive indices expected.[20]

3. Results and discussion

3.1 Light-transmission measurements

Measurements of light transmission showed that light attenuation (A) and maximum scattering (attenuation) coefficient (b) occurring in an experiment (b_{max}) show linear dependences on transmission length (l) and sample mass (m), respectively, even at high humidity settings (90% RH).

$$A = \log_{10}\left(\frac{I_0}{I}\right) = b \cdot l = b^* \cdot m \cdot l \qquad (1)$$

Based on equation (1) analogous to the Lambert–Beer law[9] they can be converted to sample-mass specific scattering coefficient values (b^*; b^*_{max}) which are independent of the two parameters. Symbols used in this relation are summarized in Table 2. Note that mass here does not refer to aerosol mass (mass concentration of particles in the chamber) but to mass of incinerated sample. Because some products remain gaseous or quickly precipitate as solid ashes, while water vapor can be absorbed by aerosol particles, mass of aerosol generated by pyrotechnics is not easily predictable, whereas sample mass is a convenient reference.

Table 2. *Variables used in the scattering relation*

Symbol	Description
A	Light attenuation
I_0	Initial light beam intensity
I	Light intensity at the detector
m	Sample mass
l	Length of light path
b	Light scattering coefficient of the aerosol (smoke)
b_{max}	Maximum light scattering coefficient
b^*	Sample-mass specific scattering coefficient
b^*_{max}	Maximum sample-mass specific scattering coefficient

Only for scattering coefficients greater than 2 m^{-1}, this relation shows a non-linear behavior (Figure 2) and mass-specific scattering coefficients decrease. Processes like coagulation and deposition, which are dependent on aerosol concentration and particle size, reduce particle numbers and thereby overall light scattering. The linear region towards lower sample mass best represents real firework displays, where aerosols are quickly dispersed over a large volume. A series of similar measurements on smoke screen compositions has been performed by Harkoma.[21] In his measurements, which were performed in a smaller chamber (0.15 m^3), scattering (extinction) coefficients much more quickly decreased after combustion than observed in this study. This may be an indication of increased coagulation

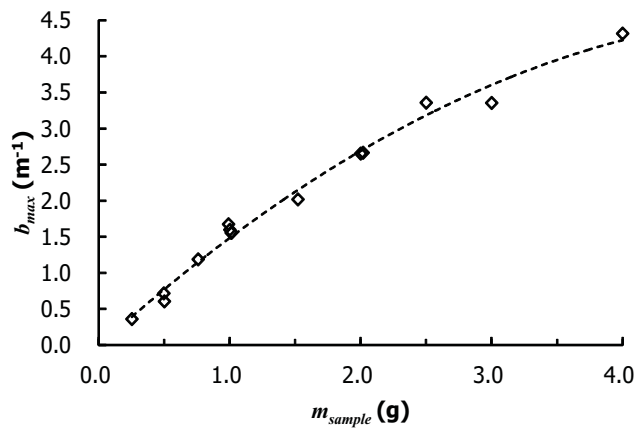

Figure 2. *Maximum scattering coefficient after combustion of composite-K at 90% RH plotted against sample mass.*

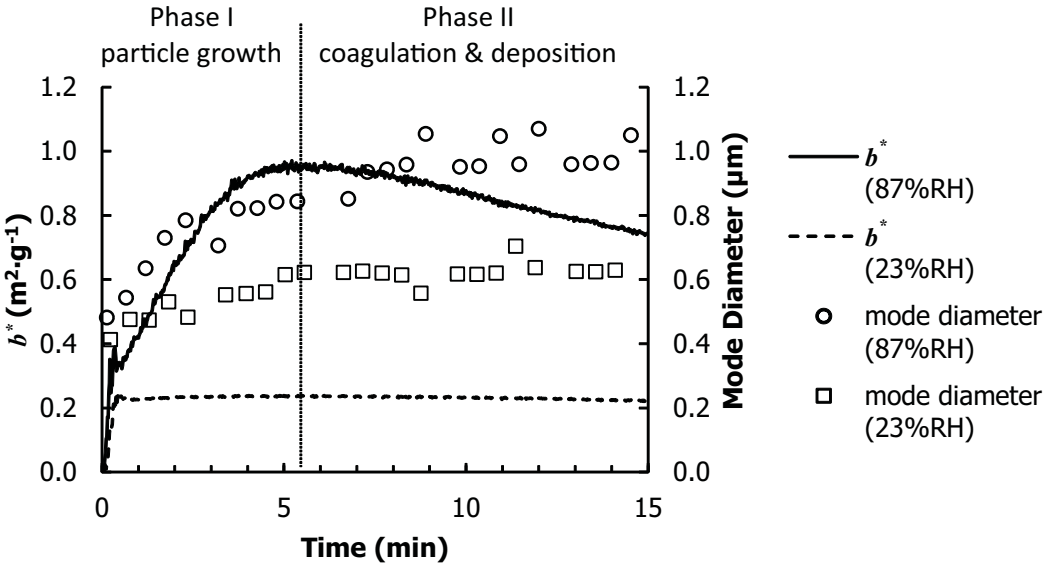

Figure 3. *b* and mode diameter of aerosol generated by combustion of 2 g composite-K at 87% RH (○) and 23% RH (□).*

and wall deposition effects. The prior is favored by higher aerosol concentrations or temperatures[22] resulting from aerosols emitted by the same amount of sample (2 g) only being diluted to a smaller chamber volume (0.15 m^3), and the latter by the chamber's higher surface-to-volume ratio.[23] Further, differences in type and resulting size distributions of the aerosols produced can also play a role.

Despite its similarity to the Beer–Lambert law, b^* gained by this relation displayed a time dependence caused by particle growth and deposition in the generated aerosol, especially at high relative humidity conditions. Composite-K shows typical characteristics as seen in time curves of b^* in Figure 3 for 87% and 23% RH. After combustion under high humidity conditions, particle growth (mode diameter: ○) was observed for 4 to 6 minutes in phase I and reached a maximum after which b^* declined slowly. Continuing growth in mode diameter of the aerosol observed in phase II suggested a coagulation processes, but increased losses due to particle deposition on wall and fan surfaces were also possible with larger particles. Under dry conditions up to 50% RH (23% in Figure 3), b^* reached a nearly constant value immediately after initial fluctuations due to fan circulation. After slight growth (mode diameter: □) in phase I the measured PSDs also remain constant, indicating negligible coagulation and deposition for particle modes up to a diameter of 0.6 µm during the experiment. Increase of aerosol visibility of Composite-K at high RH can be attributed to condensation of water vapor and HCl onto KCl particles which leads to high number concentrations of particles with diameters around 1 µm, which have high scattering coefficients.

Somewhat different results were obtained for the remaining two compositions: in experiments with composite-A, b^* either reached its maximum even more quickly within 1 minute at humid conditions (above 80% RH) and declined within 5 to 10 minutes almost to complete transparency, or, when dry conditions (below 80% RH) were applied, did not show any measurable light attenuation at all. This is because combustion products of composite A only consist of gases like CO_2, H_2O and HCl, of which the latter induces aerosol generation at high relative humidity. Although particle size could not be measured with the particle size distribution analyzer, because scattered light intensity was too low and PSD changed too quickly, visible particle depositions on chamber walls and floor were observed and hydrochloric acid could be captured in open containers containing a layer of water placed on the chamber floor. This indicates particle loss due to precipitation of large particles which cannot be sustained in a small agitated chamber. Black powder showed time curves of b^* similar to those of composite-K, only reaching its maximum more quickly 2 to 3 minutes after combustion.

3.2 Particle-size measurements

In the current series of combustion experiments, measured PSDs were mostly found to consist of a single mode. PSDs of aerosols generated by composite-K and black powder under humid conditions displayed a mode diameter shifting to larger sizes over time, indicating particle growth which may occur by coagulation of particles or absorption of water and other vapors. The absence of particle growth under dry conditions below 40% RH suggests that coagulation over a timescale of minutes can be neglected for small particles, but may play a role after particle growth to diameters in the near-µm range.

In experiments with composite-A, particle size grew so quickly that the aerosol disappeared by deposition on chamber surfaces as indicated in the previous section and measurements with the Mie scattering PSD analyzer did not succeed due to low time resolution (≈30 s) and insufficient scattering intensity.

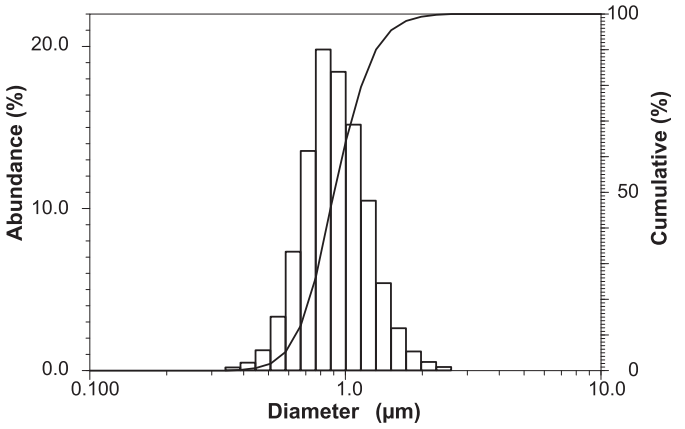

Figure 4. *Particle volume distribution of aerosol 5 minutes after combustion of 2 g composite-K at 87% RH.*

In Figure 3, mode diameter is plotted along with b^*_{max} for composite-K at 87%. Mode diameter grew from 0.55 to around 1.05 µm within a quarter of an hour, passing 0.8 µm where b^* reached its maximum. Figure 4 shows the PSD measured at that point, displaying its single mode diameter (maximum abundance). Only in a few experiments a second coarse mode of a larger particle size ranging from 4 to 9 µm could be observed because response with respect to aerosol mass was relatively low. Even larger particles are further quickly deposited before they can accumulate to sufficiently high concentrations necessary for measurement with this method.

Particles larger than 4 µm proved difficult to measure using scattered light analysis, because aerosol-mass specific light scattering intensities rapidly decrease above that size (and are lost in the light scattering background of smaller particles). In total, these particles should therefore not play a major role in aerosol visibility. For detailed analysis of large particles in such aerosols, more advanced measurement methods are required which, without further countermeasures, however, may not withstand the corrosive combustion products over prolonged times.

Supplementary measurements with an optical particle counter after combustion of very small amounts of sample as shown in Figure 5 confirmed the presence of particles exceeding diameters of 2 µm. Because the particle size resolution of the instrument used was low, the presence of multiple modes, particle size changes or precise volume concentrations, mass concentrations or diameters could not be determined with the instrument used. Volume concentrations in Figure 5 were estimated assuming spherical particles and constant number distributions in each size class.

For Composite K, particles with diameters in the range of 2–5 µm were detected, but make up only a small fraction as number concentrations. Thus they only minimally contribute to light scattering and were not detected in the measurements using the PSD analyzer. Quick disappearance of large particles formed after combustion of composite-A

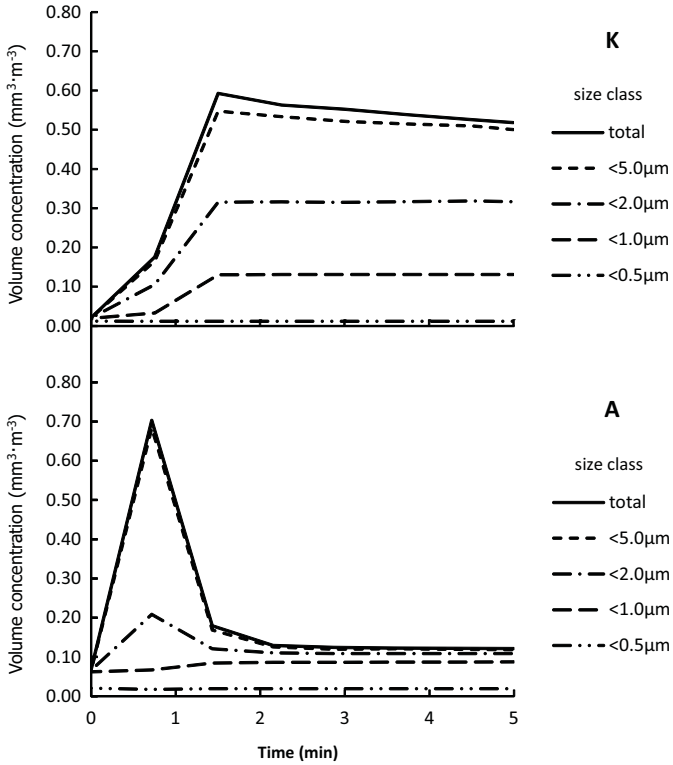

Figure 5. *Particle counter results converted to volume concentrations after combustion of 23 mg composite-K at 80% RH and 41 mg composite-A at 88% RH.*

confirmed loss of aerosol particles by deposition. Other particle measurement methods (e.g. mobility particle sizer) may provide better size resolution and enable measurement of the highly concentrated aerosols generated in chamber experiments, but require measures against particle size drifts caused by changes in relative humidity (e.g. by dilution) and corrosion of instrument parts by the combustion products.

3.3 Humidity dependence

3.3.1 Maximum mass-specific scattering coefficient

To characterize the aerosol's opacity at given conditions in simple charts, the maximum reading of b^* was extracted for each experiment. Values of b^*_{max} plotted against humidity show characteristic curves, depicting aerosol properties for each composite (Figure 6). These curves are independent of temperature and coincide for measurements performed in this study at 20 °C and 30 °C (for BP also at 10 °C). Combustion products forming solids by a phase transition from the gas-phase typically produce fine aerosol particles in the submicrometer size-range and show a base-line at dry conditions. These particles can further grow when relative humidity exceeds a characteristic threshold to form larger particles displaying higher scattering efficiencies, if they contain a hygroscopic combustion product. Critical relative humidity, at which it starts absorbing water vapor to form a liquid phase, is easily recognizable by an abrupt rise in the curve's slope and can be found in the literature for many compounds.

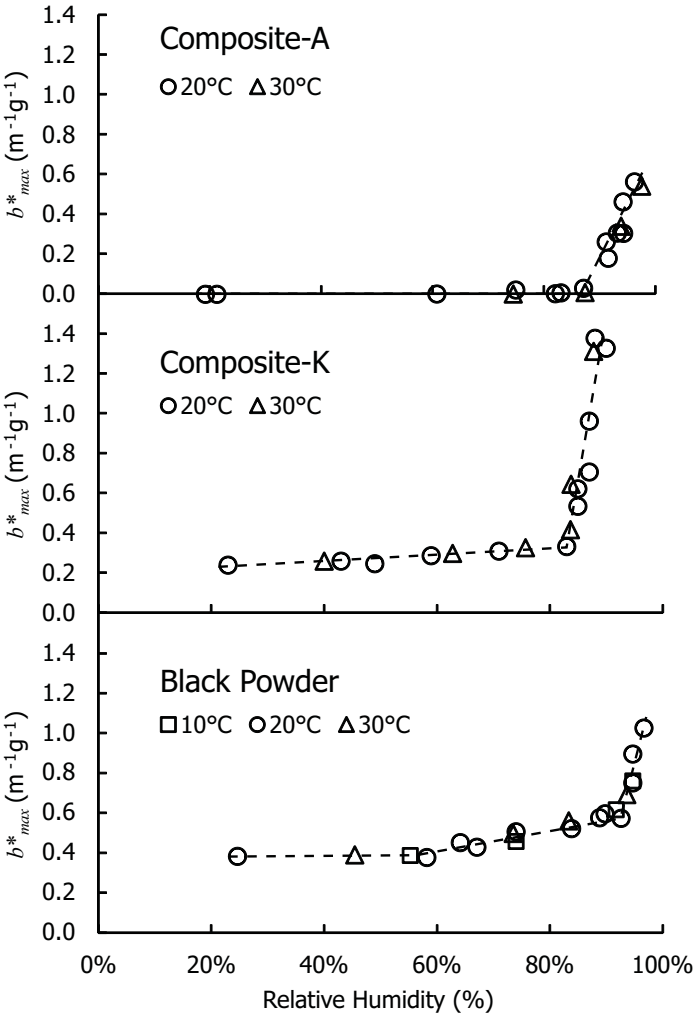

Figure 6. *b^*_{max} of composite-K, composite-A measured at 20 °C and 30 °C, of BP also at 10 °C plotted against initial relative humidity. (For composite-K values go up to 2.48 at 96% RH, but are not plotted.).*

Composite-A developed no visible aerosol at all for humidity settings below 80% RH, because its primary combustion products only consist of gases. Hydrochloric acid, one of its combustion products, produced particles which rapidly grow by absorbing water vapor at highly humid conditions causing a rise in b^*_{max}. Under experimental conditions, however, the particles grew too large to stay suspended in the confined volume of the chamber and were quickly deposited on chamber surfaces. Therefore, b^* only briefly rose and the air in the chamber cleared almost completely within a few minutes. This kind of deposition may not occur quickly in the open air. Therefore aerosols may be persistent and reach higher opacities than these measurements suggest.

Aerosols emitted by combustion of composite-K consist of KCl. Therefore, the plot of b^*_{max} is constant until critical relative humidity of KCl is reached at 85% where the plot shows a sharp rise. Unlike in composite-A, particle size does not grow so large that particles are deposited quickly.

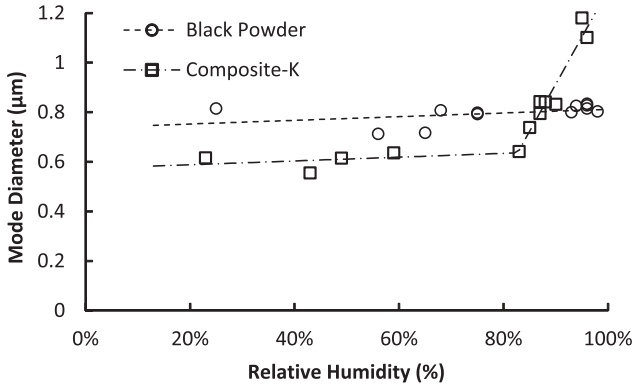

Figure 7. *Aerosol mode diameter at the time of b^*_{max} plotted against initial relative humidity.*

Combustion products of black powder consist of a complex mixture of solids and gases. Main components found in the solid fraction include K_2SO_4 and K_2CO_3, among others[24] of which only K_2CO_3 is hygroscopic with a critical relative humidity of 43%. Its high solubility and low abundance result in a moderate rise of aerosol opacity in respect to relative humidity. The final steeper rise at near saturation humidity can be attributed to K_2SO_4 (critical relative humidty: 97%).

3.3.2 Mode diameter at maximum attenuation

PSDs measured with the Mie scattering analyzer showed only a single mode for the composites measured in this work. Other modes do obviously exist, as indicated by particle counter measurements, but light scattering properties can approximately be represented by the single mode PSD measured. The size effect can be visualized more easily by plotting mode diameters of the PSDs at maximal attenuation. These plots (Figure 7) look remarkably similar to b^*_{max} (Figure 6), but rise less intensely at high humidity conditions. The significant increase in particle size from a few hundred nm to the µm-range causes the higher b^*_{max} in composite K at high RH conditions. KCl particles undergo hygroscopic growth by reduced vapor-pressure of water. For black powder, however, no rise in particle diameter is observed at all with increasing RH, although b^*_{max} clearly shows a rising tendency. Here, the main aerosol constituent K_2SO_4 does not display a simple hygroscopic growth mechanism as with composite K. The increase of b^*_{max} in this case may be indicating growth of the hygroscopic subcomponent K_2CO_3 existing as separate particles of different sizes, which could not be resolved in the presence of large amounts of K_2SO_4 particles. Also the PSD analyzer is not able to measure volume or number concentration values, which would provide more insight. To properly explain complex growth phenomena like those occurring in the example of black powder, more sophisticated measurement methods with a wider dynamic range are required.

4. Conclusions

Measurement of maximum light attenuation after combustion of pyrolant composites at controlled relative humidity conditions in an unpressurized combustion chamber were found a reproducible and handy method to characterize dependence of aerosol visibility on relative humidity. By conversion to composite-mass specific scattering coefficients, a plot independent of temperature against relative humidity can be obtained. The effect of humidity on total visible aerosol development is visualized in a simple plot and is quantitatively intercomparable between different composite types. Relative humidity limits for low smoke application can be investigated (critical relative humidity of hygroscopic combustion products) and visible aerosol development per pyrotechnic unit shot (smoke-intensiveness) can be predicted for arbitrary humidity conditions. Aerosols which were previously reported in the sub µm-range were observed to grow to diameters of around 1 µm and above by absorption of water vapor from ambient air under high relative humidity, causing aerosol opacity to increase drastically. The proposed measurement method allows effectiveness of smoke-reducing techniques in pyrotechnics to be tested in small scale experiments and can elucidate chemical components which increase visibility of aerosol emissions.

References

1 N. Kubota, "Propellant chemistry", in *Pyrotechnic Chemistry*, Journal of Pyrotechnics Inc., Whitewater, 2004, Chapter 11, pp. 7–11.

2 J. A. Conkling, "Smoke and sound", in *Chemistry of Pyrotechnics*, Marcel Dekker Inc., New York, 1985, pp. 167–179.

3 A. P. Hardt, "Generation of smoke", in *Pyrotechnics*, Pyrotechnica Publications, Post Falls, 2001, pp. 318–332.

4 D. J. Cziczo and J. P. D. Abbatt, "Infrared observations of the response of NaCl, $MgCl_2$, NH_4HSO_4, and NH_4NO_3 aerosols to changes in relative humidity from 298 to 238 K", *Journal of Physical Chemistry*, Vol. 104, 2000, pp. 2038–2047; doi: 10.1021/jp9931408.

5 A. Schenkel and K. Schaber, "Growth of salt and acid aerosol particles in humid air", *Journal of Aerosol Science*, Vol. 26, No. 7, 1995, pp. 1029–1039; doi: 10.1016/0021-8502(95)00038-E.

6 A. T. Cocks and R. P. Fernando, "The rates of formation of hydrogen chloride / water aerosols by homogeneous nucleation", *Atmospheric Environment,* Vol. 15, Number 7, 1981, pp. 1293–1299; doi: 10.1016/0004-6981(81)90323-1.

7 M. Z. Jacobson, "Particle absorption and scattering", In *Fundamentals of atmospheric modelling, second edition,* Cambridge University Press, New York, 2005, pp. 301–313.

8 C. F. Bohren and D. R. Huffman, *Absorption and scattering of light by small particles*. WILEY-VCH Verlag GmbH & Co. KGaA, Weinheim, 2004, ISBN 9780471293408.

9 P. F. Pagoria, G. S. Lee, A. R. Mitchell and R. D. Schmidt, "A review of energetic materials synthesis", *Thermochimica Acta*, Vol. 384, Number 1–2, 2002, pp. 187–204; doi: 10.1016/S0040-6031(01)00805-X.

10 D. Badgujar, M. Talawar, S. Asthana and P. Mahulikar, "Advances in science and technology of modern energetic materials: An overview", *Journal of Hazardous Materials,* Vol. 151, Number 2-3, 2008, pp. 289–305.

11 B. Wehner, A. Wiedensohler and J. Heintzenberg, "Submicrometer aerosol size distributions and mass concentration of the millennium fireworks 2000 in Leipzig, Germany", *Journal of Aerosol Science*, Vol. 31, Number 12, 2000, pp. 1489–1493.

12 Y. G. Wang, Zhuang, C. Xu and Z. An, "The air pollution caused by the burning of fireworks during the lantern festival in Beijing", *Atmospheric Environment*, Vol 41, Number 2, 2007, pp. 417–431.

13 A. Dutschke, C. Lohrer, L. Kurth, S. Seeger, M. Barthel and U. Panne, "Aerosol Emissions from Outdoor Firework Displays", *Chemical Engineering & Technology*, Vol. 34, Number 12, 2011, pp. 2044–2050; doi: 10.1002/ceat.201100080.

14 A. Dutschke, C. Lohrer, S. Seeger and L. Kurth, "Gasförmige und feste Reaktionsprodukte beim Abbrand von Indoor-Feuerwerk", *Chemie Ingenieur Technik*, Vol 81, Number 1–2, 2009, pp. 167–176; doi: 10.1002/cite.200800122

15 J. T. Hanley and E. J. Mack, "A laboratory investigation of aerosol and extinction characteristics for Salty Dog, NWC 29 and NWC 78 pyrotechnics", *Calspan Report No. 6665-M-1*, Department of the Navy Naval Air Systems Command, Washington DC, 1980. http://oai.dtic.mil/oai/ oai?verb=getRecord&metadataPrefix=html &identifier=ADA093098

16 K. L. Kosanke and B. J. Kosanke, "The chemistry of colored flame", In Pyrotechnic Chemistry, Journal of Pyrotechnics Inc., Whitewater, 2004, Chapter 9, pp. 25–49.

17 *Guide to Meteorological Instruments and Methods of Observation*, Seventh edition, World Meteorological Organization, Geneva, 2008.

18 S. Prahl, "Mie Scattering Calculator", Oregon Medical Laser Center, 2012. http://omlc.ogi.edu/calc/mie_calc.html

19 P. J. Flatau, "scatterlib", Google Project Hosting, 2011. https://code.google.com/p/scatterlib/

20 F. Peng and S. W. Effler, "Mass-specific scattering coefficient for natural minerogenic particle populations: particle size distribution effect and closure analyses", *Applied Optics*, Vol. 51, Number 13, 2012, pp. 2236–2249.

21 M. Harkoma, “Visual and Near Infrared Mass Extinction Coefficient of Five Pyrotechnic Screening Smokes”, *Journal of Pyrotechnics*, Vol. 32, 2013, pp. 67–77.

22 K. Okuyama, Y. Kousaka, Y. Kida and T. Yoshida, “Turbulent coagulation of aerosols in a stirred tank”, *Journal of Chemical Engineering of Japan*, Vol. 10, Number 2, 1977, pp. 142–147.

23 J. G. Crump, R. C. Flagan, J. H. Seinfeld, “Particle wall loss in vessels”, *Aerosol Science and Technology*, Vol. 2, Number 3, 1983, pp. 303–309.

24 I. von Maltitz, “Our present knowledge of the chemistry of black powder”, in *Pyrotechnic Chemistry*, Journal of Pyrotechnics Inc, Whitewater, 2004, Chapter 6, pp. 1–12.